Supporting Information

Flexible FeVOx Porous Nanorods on Carbon Cloth for Long-Life Aqueous Energy Storage

Experimental Section

Synthesis of CC@ $FeVO_x$ (CFV_x)

$FeVO_x$ porous nanorods on carbon cloth (CC@ $FeVO_x$, CFV_x) could be synthesized by a facile two-step method. The specific operation steps are as follows:

(1) Hydrothermal synthesis of the precursor CC@$FeVO_4 \cdot 1.1H_2O$ (CFV):

Firstly, 1.670 g of $NaNO_3$, 2.433 g of $FeCl_3$ (0.015 M) and 0.0708 g of VCl_3 (0.00045 M) were dissolved successively in the 18 mL diluted hydrochloric acid solution of pH 2.5, followed by stirring for 15 min. Secondly, a piece of pretreated carbon cloth (CC) together with the above solution was added to a 25 mL Teflon lined autoclave and placed in an electric blast oven at 120 °C for 1 h. When the hydrothermal reaction was completed, the Teflon lined autoclave was allowed to cool naturally for 8 h to recover to room temperature. Finally, the treated CC was repeatedly washed with deionized water and dried at 60 °C for 12 h to obtain the CFV.

(2) High-temperature reduction roasting of CFV:

A piece of CFV was placed into a crucible and transferred to a tube furnace, where it was roasted for 2h at 600℃ under a mixed argon-hydrogen atmosphere. Afterwards, the target CFV_x was obtained after naturally cooling. The comparison sample was the AR-CFV which was roasted at 350°C for 2h in an air atmosphere.

Materials Characterization

The phase and structure of materials were characterized by X-Ray Diffraction (XRD) using an X-ray diffractometer (TTR-Ⅲ, Rigaku, Japan). Morphologies and microstructures of materials were investigated via scanning electron microscope (SEM, JSM-6380LV, JEOL, Japan), transmission electron microscopy and high resolution transmission electron microscopy (TEM, HRTEM, Tecnai G2 F20 STWIN, Japan). A Nicolet 6700 spectrometer from Thermo Fisher was utilized to obtain Fourier transform infrared spectra (FTIR). An alpha300 R Raman spectrometer from WITec was utilized to record Raman spectra. X-ray photoelectron spectroscopy (XPS) tests were carried out by an XPS spectrometer (ESCA LAB 25, America). Nitrogen adsorption/desorption data were obtained by an automatic specific surface area adsorbent (Micromeritics ASAP 2020, America). The surface area was determined using the Brunauer–Emmett–Teller (BET) equation. Pore size distributions were evaluated by quenched solid density functional theory (QSDFT).

Electrochemical measurement

The electrochemical performances of the supercapacitor were measured by a three-electrode system. The as-prepared CFV_x, platinum net, silver/silver chloride electrode, 1 M Na_2SO_4 were utilized as the working electrode, counter electrode, reference electrode and electrolyte, respectively. The two-electrode system was employed to evaluate the electrochemical performances of zinc-ion batteries. The as-prepared CFV_x, zinc sheet, 1 M $ZnSO_4$ were utilized as the working electrode with mass loading of 0.97-1.03 mg cm^{-2}, counter electrode and electrolyte, respectively. The galvanostatic charge/discharge (GCD) measurements, rate and cycling stability of electrodes were performed by a LAND CT2001A test system at room temperature. Cyclic voltammetry curves were obtained through a CHI760E electrochemical workstation.

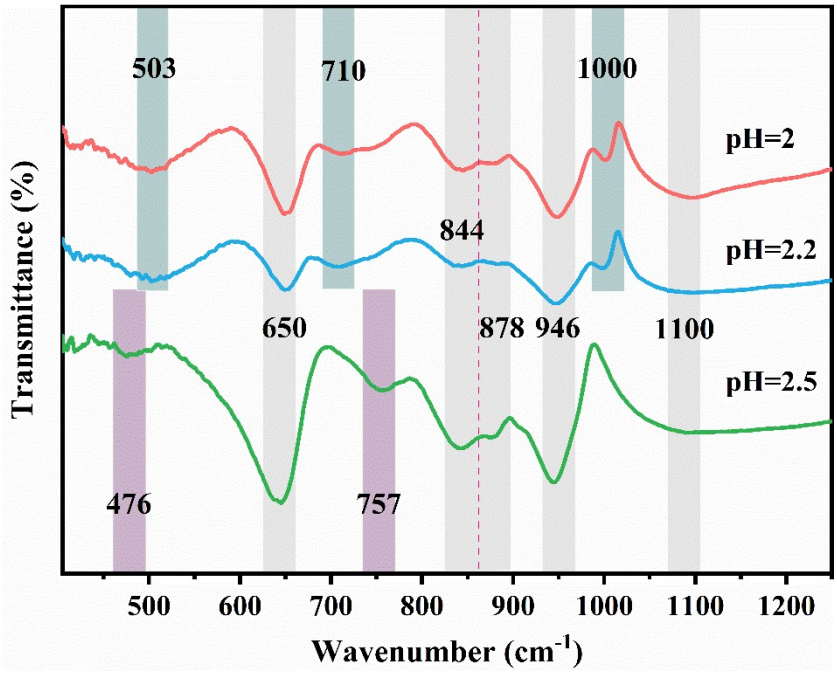

Fig. S1. The FTIR spectrum of CFV synthesized at different pH. (2, 2.2, 2.5).

During the preparation of CFV, the factors influencing its synthesis were explored. The FTIR spectrum of CFV synthesized at different pH is shown in Fig. S1. The absorption peaks at 650, 844, 878, 946 cm^{-1} which correspond to $FeVO_4 \cdot 1.1H_2O$ were observed from all samples. According to the literature, the peaks at 650, 844, 878 cm^{-1} are attributed to the stretching vibration of V-O-Fe, and the peak at 946 cm^{-1} is assigned to the stretching vibration of V-O.[1] The spectrum of CFV synthesized at pH 2 and 2.2 contained heterogeneous peaks at 710 and 1000 cm^{-1} originating from $Fe_5V_{15}O_{39}(OH)_9 \cdot 9H_2O$.[S1, 2] These results indicate that the purity of CFV synthesized at different pH varied, with a higher purity at pH=2.5.

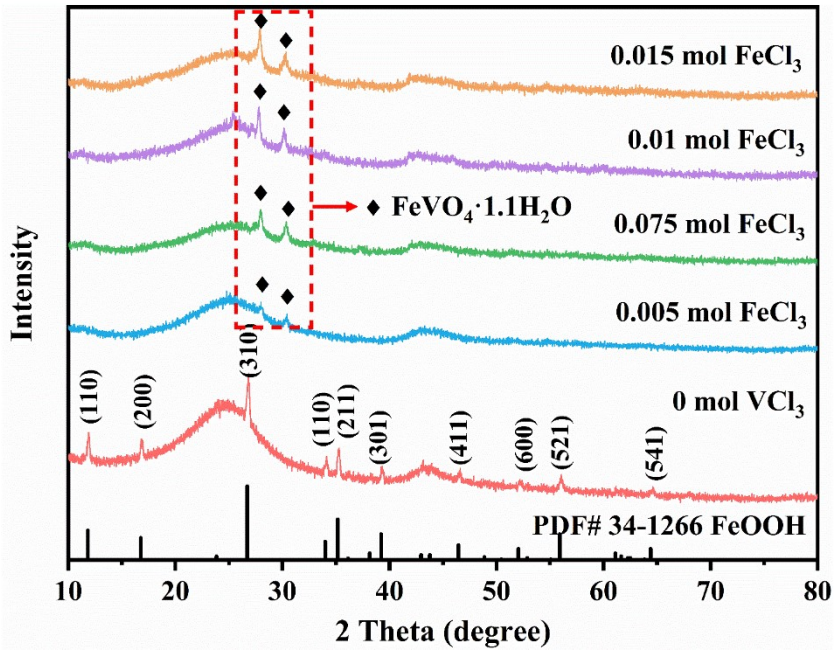

Fig. S2. The XRD of CFV synthesized at different amount of $FeCl_3$ added.

As shown in Fig. S2, the diffraction peaks at 27.8° and 29.4° indexed into $FeVO_4 \cdot 1.1H_2O$ could be observed from all samples,[3] indicating that an appropriate adjustment in Fe ion concentration does not affect the crystal structure of the phase. However, the peak intensity increased with increasing Fe ion concentration, suggesting that higher $FeCl_3$ additions are beneficial in improving the loading of this material. It is also worth noting that only FeOOH was produced when no VCl_3 was added.

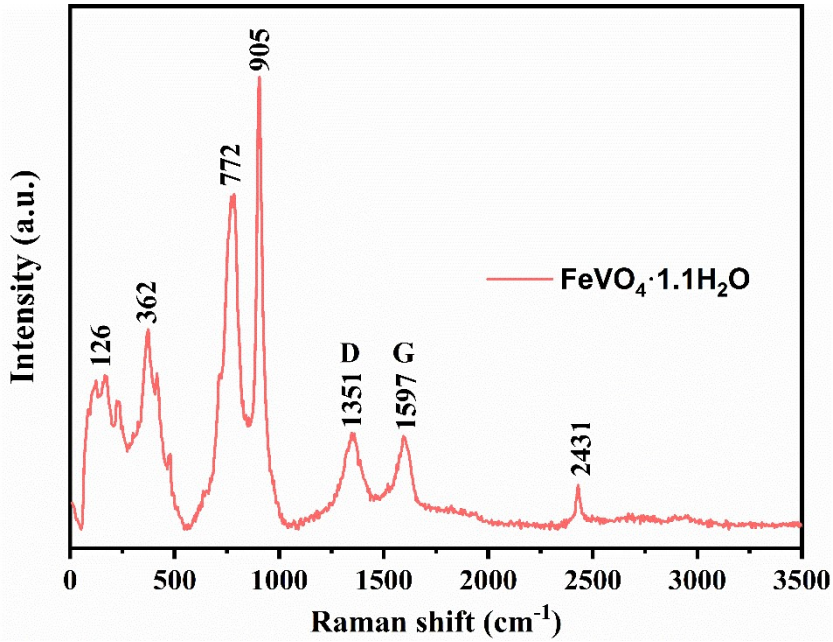

Fig. S3. The Raman spectroscopy of CFV.

The successful loading of $FeVO_4 \cdot 1.1H_2O$ was further demonstrated by Raman spectroscopy, as shown in Fig. S3. Both the characteristic peaks[1] from 0 to 1000 cm^{-1} and the D/G peaks of CC at 1351/1597 cm^{-1} were detected from the CFV electrode, with the peak at 2431 cm^{-1} corresponding to the atmospheric nitrogen.[S4]

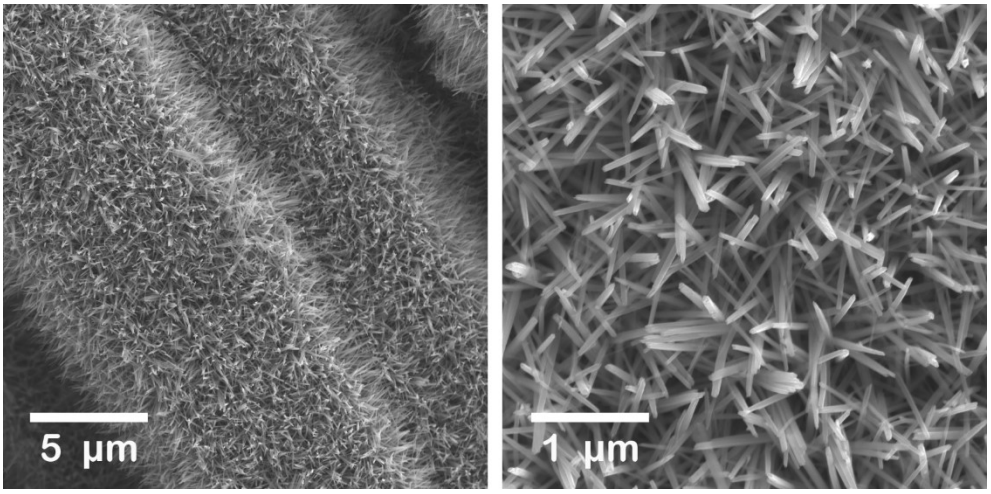

Fig. S4. The SEM images of CFV.

Fig. S4 displays the SEM images of CFV, showing that the $FeVO_4 \cdot 1.1H_2O$ nanorods were uniformly loaded on the CC at the condition of pH=2.5, 0.015 M $FeCl_3$, 3% VCl_3.

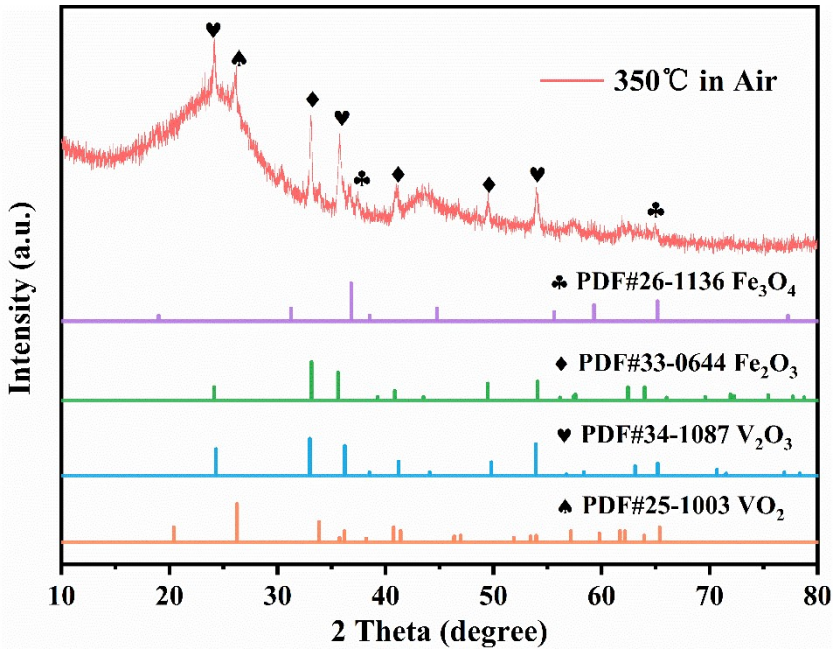

Fig. S5. The XRD pattern of AR-CFV.

As shown in Fig. S5, after air roasting at 350°C for 2 h, the $FeVO_4 \cdot 1.1H_2O$ coated on CC will transform into a mixture of oxides, including Fe_3O_4, Fe_2O_3, V_2O_3 and VO_2.

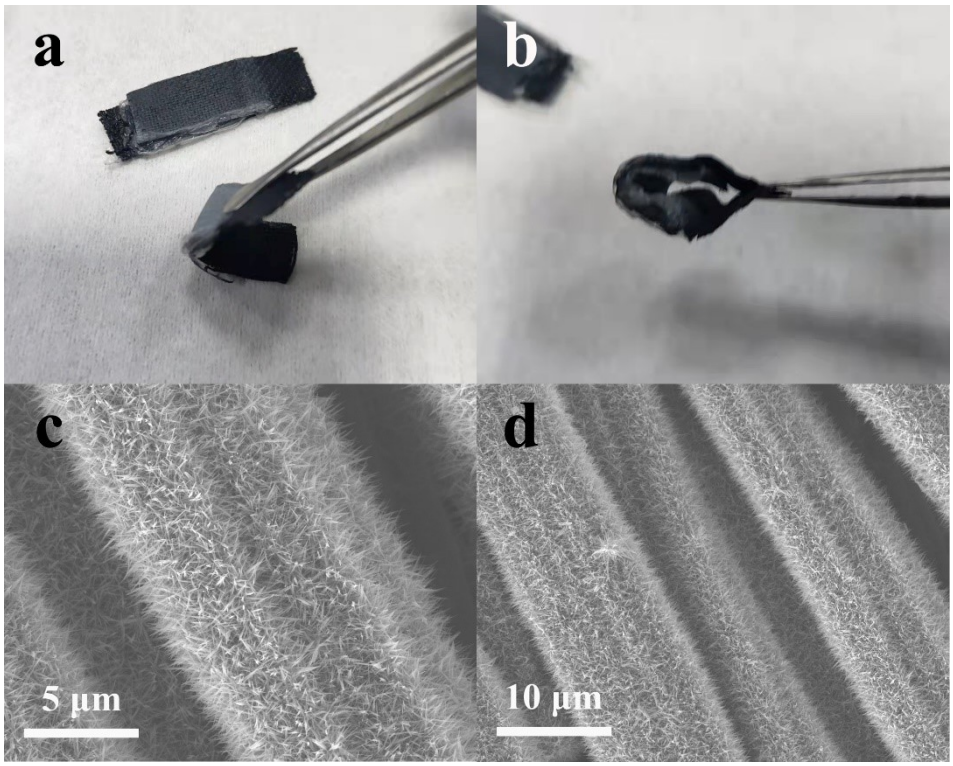

Fig. S6. The images of CFV_x electrode bending at (a) 90° and (b) 180°. SEM images of CFV_x after several bends (c,d).

As shown in Fig. S6a and b, the synthesized electrode CFV_x can be bent through 90° and 180°. Furthermore, according to the SEM images (Fig. S6c and d) of the CFV_x after several bends, the porous nanorods on the carbon cloth fibers still maintain a remarkable structural stability, demonstrating that CFV_x possesses an outstanding mechanical flexibility.

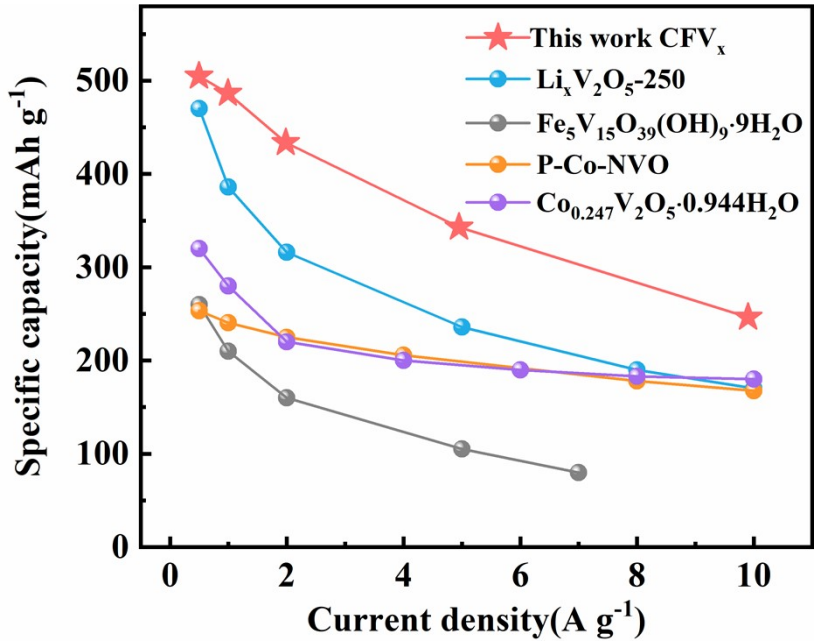

Fig. S7. The comparison of specific capacities between CFV_x electrode and previously reported electrodes.

As shown in Fig. S7, the CFV_x electrode for ZIBs shows superior electrochemical performances comparing to the reported vanadium-based materials.[S5-S8]

Table S1. Atomic ratio of elements C, O, V, Fe (via EDS mapping)

Element	*Wt%*	*At%*
CK	76.33	89.92
OK	06.14	05.43
VK	08.56	02.38
FeK	08.97	02.27
Matrix	Correction	MThin

References

S1. T. Lehnen, M. Valldor, D. Nižňanský and S. Mathur, *J. Mater. Chem. A*, 2014, **2**, 1862-1868.

S2. C. Liu, Z. Neale, J. Zheng, X. Jia, J. Huang, M. Yan, M. Tian, M. Wang, J. Yang and G. Cao, *Energy Environ. Sci.*, 2019, **12**, 2273-2285.

S3. C. Yang, F. Lv, Y. Zhang, J. Wen, K. Dong, H. Su, F. Lai, G. Qian, W. Wang, A. Hilger, Y. Xu, Y. Zhu, Y. Deng, W. Hu, I. Manke and Y. Chen, *Adv. Energy Mater.*, 2019, **9**, 1902674.

S4. R. Escribano, J. J. Sloan, N. Siddique, N. Sze and T. Dudev, *Vib. Spectrosc.*, 2001, **26**, 179-186.

S5. Y. Yang, Y. Tang, G. Fang, L. Shan, J. Guo, W. Zhang, C. Wang, L. Wang, J. Zhou and S. Liang, *Energy Environ. Sci.*, 2018, **11**, 3157-3162.

S6. M. Du, Z. Miao, H. Li, F. Zhang, Y. Sang, L. Wei, H. Liu and S. Wang, *Nano Energy*, 2021, **89**, 106477.

S7. L. Ma, N. Li, C. Long, B. Dong, D. Fang, Z. Liu, Y. Zhao, X. Li, J. Fan, S. Chen, S. Zhang and C. Zhi, *Adv. Funct. Mater.*, 2019, **29**, 1906142.

S8. Z. Peng, Q. Wei, S. Tan, P. He, W. Luo, Q. An and L. Mai, *Chem. Commun.*, 2018, **54**, 4041-4044.